11,12

Formation of catalyst nanoparticles for the growth of carbon nanotubes during annealing of amorphous Co-Zr-O films

© S.V. Bulyarskiy[1], P.E. L'vov[1,2], A.A. Pavlov[1], A.V. Terentiev[3]

[1] Institute of Nanotechnology of Microelectronics, Russian Academy of Sciences, Moscow, Russia
[2] Ulyanovsk State University, Ulyanovsk, Russia
[3] Moscow Institute of Electronics and Mathematics, High School of Economics, Moscow, Russia

E-mail: bulyar2954@mail.ru

Received June 2, 2022
Revised June 2, 2022
Accepted June 12, 2022

The formation of nanosized catalyst particles for the growth of carbon nanotubes can be carried out during the crystallization of amorphous films consisting of two metals, one of which has higher free energy of the oxide. During annealing in the presence of oxygen, this metal is oxidized with the reduction of the second metal, which leads to the formation of nanoparticles embedded in the oxide of the first metal. This the process has been experimentally and theoretically studied by the example of the formation of cobalt nanoparticles on the surface of amorphous Co-Zr-O films as a result of the decomposition of a supersaturated solid solution and mechanical stresses arising during the oxidation of zirconium. We have proposed a mechanism for the formation of catalyst nanoparticles and phenomenological model of this process developed on the basis of the phase-field theory.

Keywords: carbon nanotubes, nanoparticles of catalyst, phase transitions, decomposition of supersaturated solid solutions.

DOI: 10.21883/0000000000

1. Introduction

Vertical arrays of carbon nanotubes grown on silicon planar substrates are used in various electronic devices. Carbon nanotubes in such arrays must have a small scatter of their diameters and must chiefly have no bends. Selection and technology for preparing catalyst nanoparticles on a planar substrate are important for the attainment of these parameters. Such nanoparticles determine the main nanotube characteristics: perfection of graphene planes, their generatrices, formation of tube bends, array diameter, length and growth rates [1,2]. One of the main shortcomings of nanoparticles, forming during melting of thin catalyst metal films, is a large dispersion of nanoparticle size distribution and the coalescence phenomenon which leads to a change of particle sizes directly during CNT synthesis. Thereat, synthesized nanotubes also have a large scatter of diameters and bends. Both factors adversely affect the device quality. This shortcomings can be eliminated by developing other technologies for nanoparticle formation, including with the use of mesoscopic nanoporous materials for the formation of catalyst nanoparticles [3–5]. The result is porous oxide systems and catalyst nanoparticles are located in these pores. This approach has several shortcomings for the planar technology. Firstly, the technology for the formation of such catalysts is rather complex, it comprises several stages which can cause contamination of the planar substrate where an integrated circuit is formed. Secondly, a metal nanoparticle is immersed in an oxide which is usually a dielectric and poorly conducts electrical current, which restricts its application in the making of nanoelectronic elements.

These shortcomings can be eliminated by using catalysts based on the phenomena of decomposition of supersaturated solid solutions [7–10]. Such catalysts are made by depositing a thin amorphous film onto a substrate; the film is a solid solution of an oxide or an oxynitride with a dissolved transition metal, which acts as a catalyst of carbon nanotube growth. Heating of the film leads to the decomposition of the supersaturated solid solution, which results in the formation of catalyst nanoparticles. The advantage of such catalysts over the mesaporous ones is the higher conductivity of the catalyst layer. The goal of the present paper is justification of the mechanism of formation of catalyst particles under decomposition of supersaturated solid solutions based on the experimental data obtained for amorphous Co-Zr-O films, as well as creation of a theoretical model to describe this process.

2. Experimental results

Samples on a silicon planar substrate were made for the study of formation of catalyst particles from amorphous Co-Zr-O films. Thin films of this material were made by simultaneous electron-beam deposition of cobalt and zirconium from two crucibles. Electron beam power was selected so that the film composition corresponded to 30%

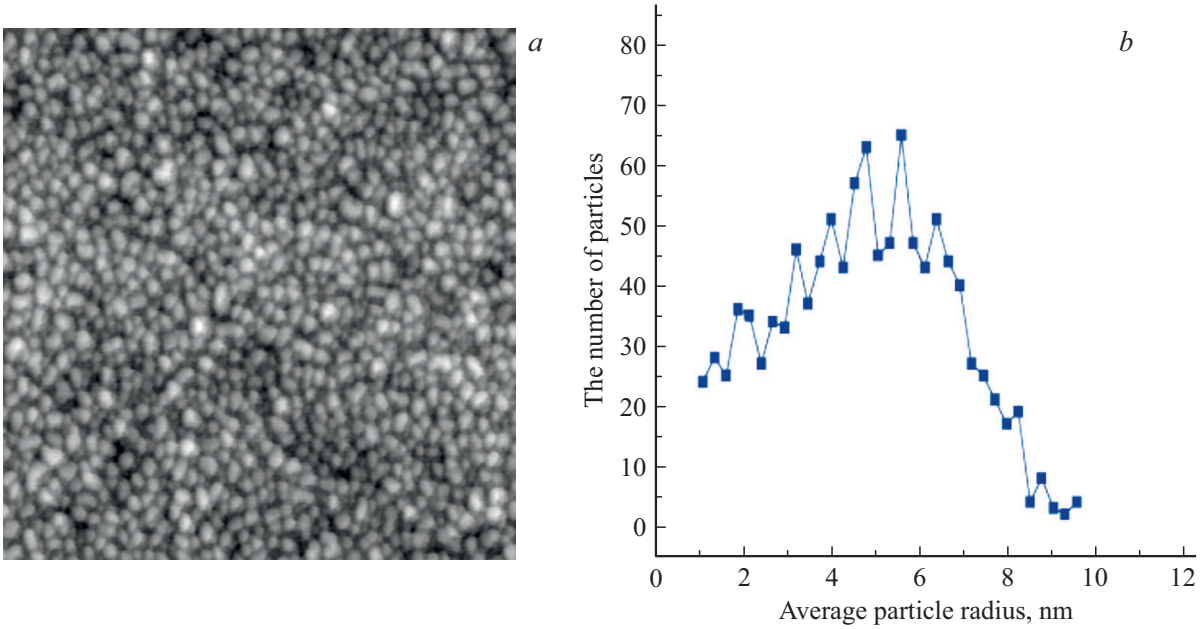

Figure 1. Image of the film surface in atomic-force microscope (*a*) and nanoparticle distribution by radius value (*b*).

of cobalt and 70% of zirconium. The oxygen flow rate in the reactor, during evaporation of metals, was 5 sccm. The film thickness was from 25 to 30 nm.

The films were annealed. The first annealing stage (oxidation) was performed at 280°C for 5 minutes in oxygen plasma excited by a high-frequency discharge with the power of 30 W. The second annealing stage (reduction) was performed in argon and ammonia atmosphere at 700°C for 5 minutes. Carbon nanotubes were synthesized in a 30 : 20 : 100 mixture of acetylene, ammonia and argon at 700°C for 10 minutes. The array of carbon nanotubes obtained by this technology consisted of vertical, well-oriented nanotubes with a diameter of 8 to 14 nm. Later on, in order to analyze the formation of catalyst nanoparticles, we imitated the synthesis process with the duration of the second stage of 15 minutes and without acetylene in the reactor.

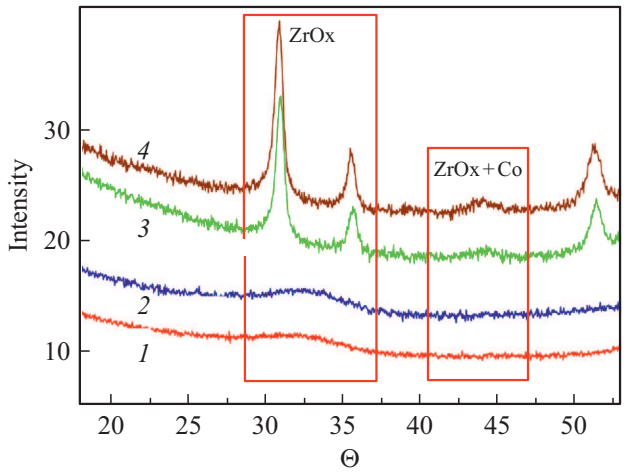

Figure 2. Results of X-ray diffraction analysis of the first batch of samples: *1* — initial, *2* — oxidized, *3* — reduced 5 min, *4* — reduced 15 min.

An image of the catalyst surface after the second stage was obtained using an atomic-force microscope and is shown in Fig. 1. Catalyst particles are clearly confined and have a narrow dispersion of distribution by an average radius value. Particle diameter corresponds to the diameter of nanotubes formed from them.

The film phase composition before and after the formation by catalyst nanoparticles was studied by the X-ray diffraction analysis method. The initial samples, right after film application, are X-ray amorphous. The film crystallizes during annealing at 700°C. Thus, annealing at 700°C results in the decomposition of the X-ray amorphous solid solution with the formation of zirconium oxide and metal cobalt. Metal cobalt rises to the surface in the form of catalyst nanoparticles which have a high homogeneity and a narrow distribution dispersion (Fig. 2).

The distribution dispersion during annealing does not change and the coalescence phenomenon is not observed, as distinct from nanoparticle formation during melting of a thin catalyst metal film.

3. Phenomenological model of formation of catalyst nanoparticles during crystallization of amorphous films

We will analyze the particle formation process using the phenomenological approaches of the phase field theory [10]. According to the basic concept of this approach, we introduce a set of non-conservative order parameters η_i, each of which corresponds to a certain grain orientation

in relation to the chosen direction [11–16]. As a rule, a few tens of order parameters are considered, while dynamics of each of them is considered using the Ginzburg–Landau equation. This approach is widely used to analyze the grain formation and growth both in single-phase [11] and in two-phase systems [12–16]. This phenomenological approach makes it possible to calculate the grain growth dynamics, determine the size distribution functions, as well as to obtain data about the nature of formation of grain boundaries and junctions, which to a great degree determine the material's mechanical and electric properties.

The main peculiarity of the Co-Zr-O system and similar systems is a change of film volume upon an amorphous-crystalline transition. Thereat, mechanical stresses arise in it. This process is revealed in experiments by certain cracking of the film. Thus, the amorphous Co-Zr-O film crystallizes during annealing and the forming grains are depleted (Zr-O) and rich in the dissolved component (Co). We will characterize the grains using order parameters η_i^α and η_i^β, where indices α and β refer to the cobalt-rich and depleted phases, respectively. These order parameters have a value equal to 0 in the amorphous state and ± 1 in the crystallized state. Using the basic approaches of the phase field theory [10–12], we will note down the free energy density functional as

$$F = \int_V \left[f\left(\xi, c, \{\eta_i^\alpha\}, \left\{\eta_i^\beta\right\}\right) + \frac{\kappa_\xi}{2}(\nabla\xi)^2 + \frac{\kappa_c}{2}(\nabla c)^2 + \frac{\kappa_\alpha}{2}\sum_i (\nabla\eta_i^\alpha)^2 + \frac{\kappa_\beta}{2}\sum_i \left(\nabla\eta_i^\beta\right)^2 \right] dV, \tag{1}$$

where ξ is the order parameter proportional to the substance concentration, which is equal to 1 in the solid state and 0 in the outside environment, c is concentration field corresponding to cobalt distribution in the system, κ_ξ, κ_c, κ_η^α, κ_η^β are gradient energy coefficients.

Assuming an approximation of regular solutions (mixtures), free energy density in a system with a variable value of order parameter ξ can be presented as

$$\begin{aligned} f(\xi, c, \{\eta_i^\alpha\}, \{\eta_i^\beta\}) &= \frac{1}{2}W\xi^2(1-\xi)^2 + \Omega(\xi)c(1-c)\xi^2 \\ &+ k_B T\left[\xi c\ln(\xi c) + (1-c)\xi\ln\left(\xi(1-c)\right)\right] \\ &- \frac{a_\alpha}{2}\xi^4(1-c)^2\sum_i(\eta_i^\alpha)^2 - \frac{a_\beta}{2}\xi^4 c^2\sum_i\left(\eta_i^\beta\right)^2 \\ &+ \frac{b_\alpha}{4}\xi^4\sum_i(\eta_i^\alpha)^4 + \frac{b_\beta}{4}\xi^4\sum_i\left(\eta_i^\beta\right)^4 + \xi^4\frac{d_{\alpha\beta}}{2}\sum_{ij}(\eta_i^\alpha)^2(\eta_j^\beta)^2 \\ &+ \xi^4\frac{d_{\alpha\alpha}}{2}\sum_{i\neq j}\left(\eta_i^\alpha\right)^2\left(\eta_j^\alpha\right)^2 + \xi^4\frac{d_{\beta\beta}}{2}\sum_{i\neq j}\left(\eta_i^\beta\right)^2\left(\eta_j^\beta\right)^2, \end{aligned} \tag{2}$$

where W is the interaction parameter for order parameter ξ, $\Omega(\xi) = \Omega_S h(\xi) + \Omega_G(1-h(\xi))$ — interaction parameter in the solution ($\xi = 1$, Ω_S) or gas phase ($\xi = 0$, Ω_G), $h(\xi)$ is smooth approximating function $h(\xi) = \xi^2(3-2\xi)$, a_i, b_i, d_{ij} $(i, j = \alpha, \beta)$ are interaction parameters for order parameters which describe crystallization. In formula (2) and further we imply summation by all indices i and j, the values of which are from 1 to P_α and P_β, respectively.

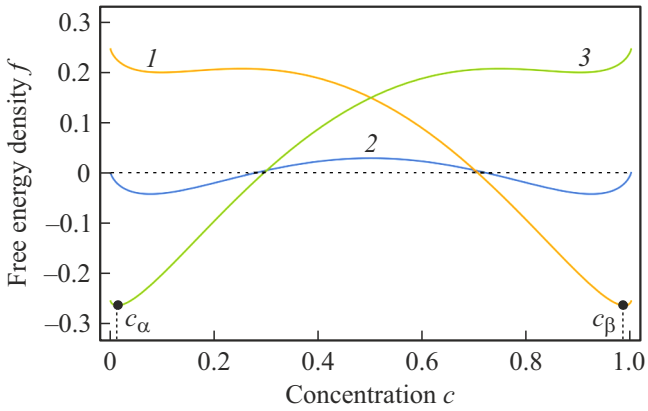

Figure 3. Free energy density f vs. concentration c for crystallized and amorphous phases ($\xi = 1$, $T = 0.68$, $\Omega_G = 2.8$, $W = 10.0$, $a_\alpha = a_\beta = 1.0$, $b_\alpha = b_\beta = 0.98$). The solid lines show the dependences for different states: *1* — cobalt-rich crystallized phase ($\eta_1^\beta = 1$, $\eta_i^\beta = 0$ at $i > 1$; $\eta_i^\alpha = 0$ for all i), *2* — amorphous phase ($\eta_i^\alpha = 0$, $\eta_i^\beta = 0$ for all i), *3* — cobalt-depleted crystallized phase ($\eta_1^\alpha = 1$, $\eta_i^\alpha = 0$ at $i > 1$; $\eta_i^\beta = 0$ for all i). Concentration values c_α and c_β correspond to cobalt-depleted and cobalt-rich equilibrium compositions of grains, respectively.

An important peculiarity of free energy density (2) is the presence of extreme values for a multitude of order parameters η_i^α and η_j^β, where only one of the parameters is equal to 1 or -1, while all the others are zero, which makes it possible to observe the formation of separated grains characterized by their own (non-zero) order parameter [11–13].

The dependences of free energy density which explain the formation of cobalt-rich and cobalt-depleted grains are shown in Fig. 3. The figure shows that the system state is the most stable when the forming grains are characterized by compositions c_α and c_β. It is also evident that the amorphous phase, which is concentrated near the grain boundaries after crystallization, is energetically unfavorable, therefore its fraction must have the tendency to decrease. Grain boundaries are also characterized by a positive interaction energy, described by parameters d_{ij} (see formula 2), which causes a surface tension at the boundaries. Thus, grain boundaries, as structure defects which cause an increase of system energy, are energetically unfavorable. Due to this, a system must evolve towards a decrease of the grain boundary region, which is attained when the grain size increases.

Order parameter ξ (actually it is the particle count in volume unit) and cobalt concentration c are the persistent order parameters, while η_i^α and η_i^β are the non-persistent

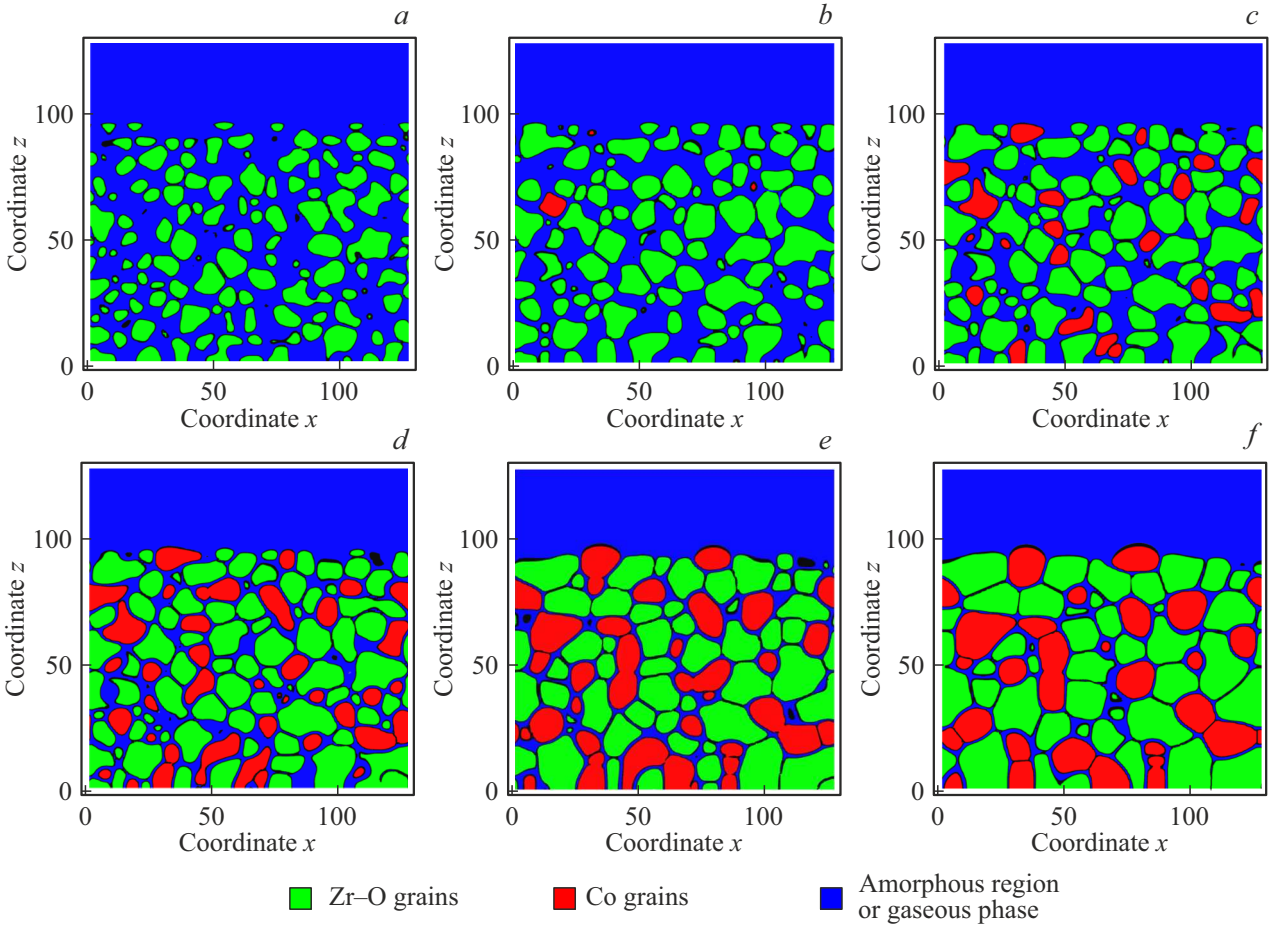

Figure 4. Dynamics of grain formation and growth in the film. The figures correspond to different time moments t: (a) — 55, (b) — 105, (c) — 130, (d) — 155, (e) — 305, (f) — 500. The grains are shown as constant-value surfaces of order parameters $\phi_\alpha = 0.7$ and $\phi_\beta = 0.7$.

order parameters, then the equations which describe their dynamics can be obtained using the continuity equation and the introduced free energy density functional (1):

$$\frac{\partial \xi}{\partial t} = \nabla\left[M_\xi \nabla\left(\frac{\delta F}{\delta \xi}\right)\right] = \nabla\left[M_\xi \nabla\left(\frac{\partial f}{\partial \xi} - \kappa_\xi \nabla^2 \xi\right)\right],$$

$$\frac{\partial c}{\partial t} = \nabla\left[M_c \nabla\left(\frac{\delta F}{\delta c}\right)\right] = \nabla\left[M_c \nabla\left(\frac{\partial f}{\partial c} - \kappa_c \nabla^2 c\right)\right],$$

$$\frac{\partial \eta_i^\alpha}{\partial t} = -M_\alpha\left(\frac{\delta F}{\delta \eta_i^\alpha}\right) = M_\alpha\left(\kappa_\alpha \nabla^2 \eta_i^\alpha - \frac{\partial f}{\partial \eta_i^\alpha}\right),$$

$$i = 1 \ldots P_\alpha,$$

$$\frac{\partial \eta_i^\beta}{\partial t} = -M_\beta\left(\frac{\delta F}{\delta \eta_i^\beta}\right) = M_\beta\left(\kappa_\beta \nabla^2 \eta_i^\beta - \frac{\partial f}{\partial \eta_i^\beta}\right),$$

$$i = 1 \ldots P_\beta. \qquad (3)$$

Here M_ξ, $M_c(\xi)$, M_a, M_β are mobilities. The equations in relation to c and ξ correspond to the Cahn–Hilliard equation, while the equations in relation to η_i^α and η_i^β are non-steady-state Ginzburg–Landau equations. The measurement units for temperature and phenomenological parameters of the model were taken equal to

$$[T] = T_C, \quad [\Omega] = k_B T_C, \quad [\mathbf{r}] = [l],$$

$$[\kappa] = 2k_B T_C l^2, \qquad [t] = M_c k_B T_C / l^2,$$

where l is correlation length usually estimated as a value equal to several lattice constants.

The differential equation system (3) was solved numerically using the finite difference method [17], which is rather efficient when solving non-linear diffusion equations. It was solved for a system sized $128l \times 128l \times 128l$. The number of the considered order parameters, corresponding to the forming cobalt-rich and cobalt-depleted phases, was $P_\alpha = 28$, $P_\beta = 28$.

The phenomenological interaction parameters were taken equal to: $T = 0.68$, $\Omega_G = 2.8$, $\Omega_S = 2.0$, $W = 10.0$, $\kappa_c = \kappa_\alpha = \kappa_\beta = 0.5$, $\kappa_\xi = 3.0$, $a_\alpha = a_\beta = 1.0$, $b_\alpha = b_\beta = 0.98$. At the initial time moment, the system consisted of a solid phase and a gas phase, and their interface had the coordinate $z = 96$. Below the said boundary there was an amorphous film which contained

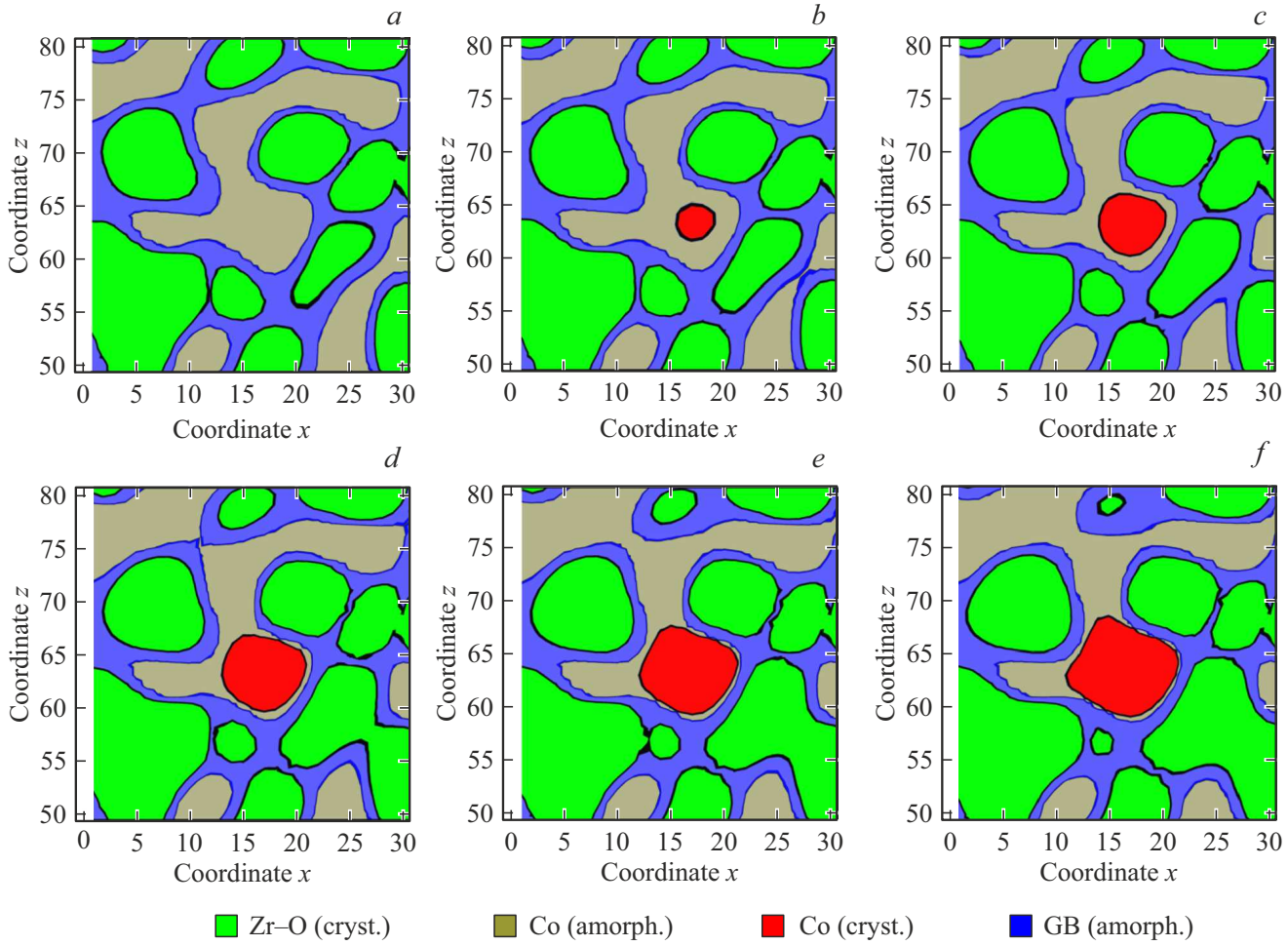

Figure 5. Dynamics of formation of a cobalt-rich grain (red color). The other colors show: blue color — amorphous region, green — cobalt-depleted grains, gray — cobalt-rich amorphous region. The figures correspond to different time moments t: (a) — 80, (b) — 85, (c) — 90, (d) — 95, (e) — 100, (f) — 105. Grains are shown as constant-value surfaces of order parameters $\phi_\alpha = 0.7$ and $\phi_\beta = 0.7$.

cobalt (distributed throughout the film volume) with the total overall concentration of $\langle c \rangle = 0.3$, which corresponds to the unstable state region where activationless formation of second phases (spinodal decomposition) can be observed. The initial film was in the amorphous state, which corresponds to the average values of order parameters $\langle \eta_i^\alpha \rangle = 0$ and $\langle \eta_i^\beta \rangle = 0$ throughout the volume occupied by the film. The concentration of the dissolved component in the initial gas phase was small and taken equal to 0.012. The order parameter in the amorphous film was taken equal to $\xi = 0.8$, and in the gas phase it was $\xi = 0.01$. The concentration field, as well as order parameters at the initial time moment were characterized by small Gaussian fluctuations with dispersion $\sigma^2 = 10^{-4}$.

Grain distribution over the system volume was recorded using parameters $\phi_\alpha = \Sigma_i \eta_i^{\alpha^2}$ and $\phi_\beta = \Sigma_i \eta_i^{\beta^2}$, which were further used for the visualization of the distribution of different grain types over the system volume.

The dynamics of grain formation and growth in the initial amorphous film was obtained by solving equation system (2). The modeling results are shown in Figs. 4–6. The considered phenomenological model parameters are characterized by the following sequence of formation of catalyst particles on the film surface. Cobalt-depleted grains form in the beginning of annealing of the initial film (Fig. 4, a, 5, a). During their formation, cobalt is displaced into the intergrain region due to the movement of the crystallization front. Cobalt concentration becomes rather high and a cobalt-rich amorphous phase forms by the spinodal mechanism (Fig. 5, a). Cobalt-rich regions gradually undergo an amorphous-crystalline transition with the formation of nanoparticles (Fig. 5, a–d). Cobalt nanoparticles actually form by a two-stage mechanism: the formation of an enriched amorphous phase and its subsequent crystallization (also see [18]). The result is a system consisting of alternating grains of different types (Fig. 4, c–f). Large grains grow and small grains disappear (Fig. 4, d–f).

The considered interaction parameters are characterized chiefly by triple grain junctions, which is usually associated with the most stable configuration [11]. The formation of quadruple junctions is observed rather rarely and, to a

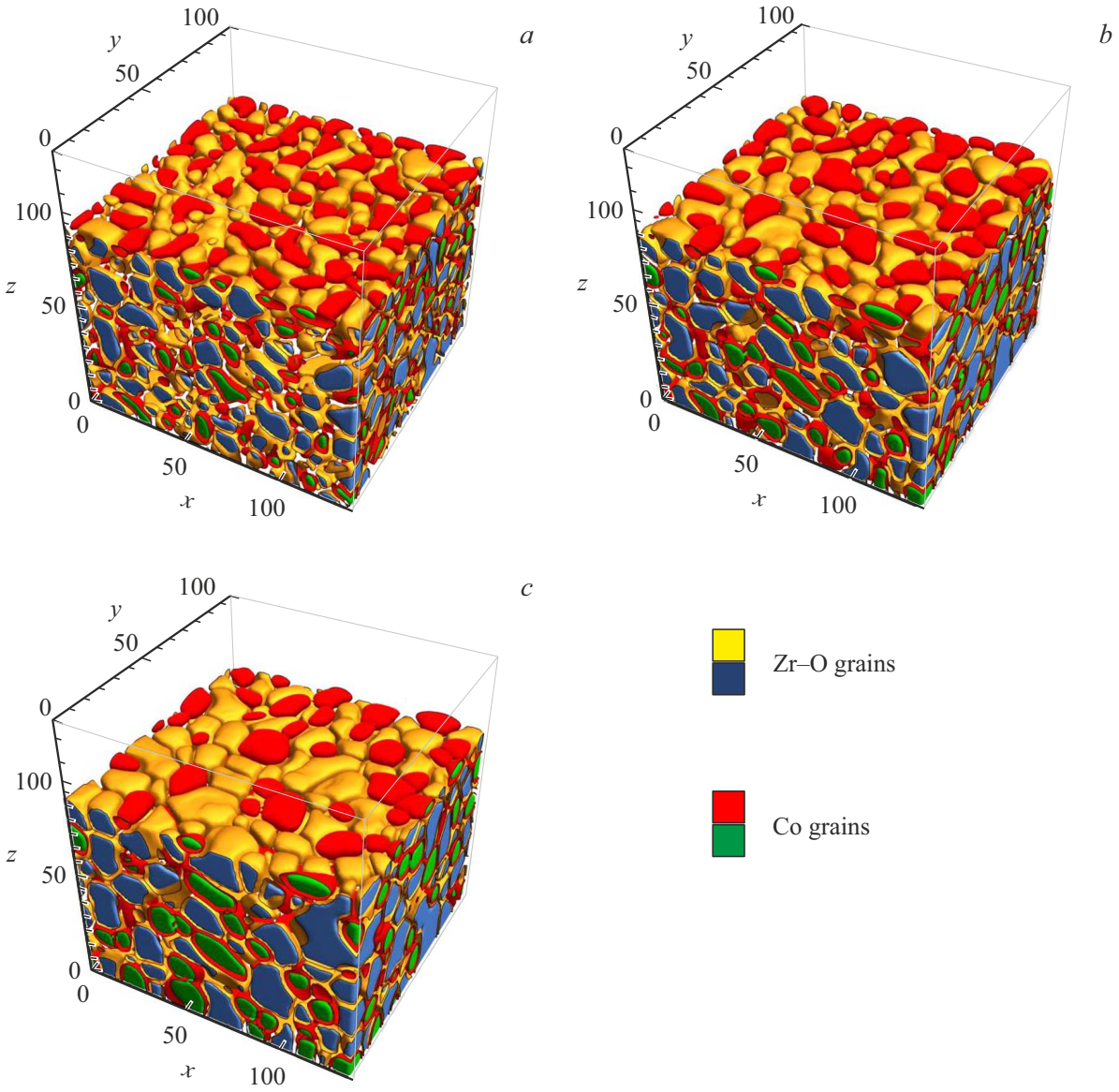

Figure 6. Results of modelling of film recrystallization (Co-Zr-O) with the formation of catalyst particles (Co) on the particle surface. The figures correspond to different time moments: *a* — 155, *b* — 305, *c* — 500.

greater degree, is a short-time process of system relaxation after the disappearance of small grains or fusion of large grains having the same orientation.

The possible mechanisms of increase of the average grain size at the final stage are the Ostwald and Smoluchowski mechanisms. When grains having the same orientation are near each other, they fuse to form a larger grain. This grain coarsening process is observed both for the grains in the film bulk and for the grains on the surface. On the whole, fusions of grains having the same orientation are rather rare due to the low probability of formation of such grains near each other. The fusion of catalyst particles (Smoluchowski ripening) on the surface virtually does not occur due to several reasons. Firstly, the concentration of catalyst particles on the surface is small, due to which their lateral interaction is rare. Secondly, catalyst particles are partially immersed in the film and surrounded chiefly by cobalt-depleted grains (Fig. 4, *e,f*). Thirdly, most catalyst particles which are near each other have a different crystal lattice orientation, i.e., their interface has energy and does not prevent their direct fusion (Fig. 6, *b, c*). Thus, the change of the film nanostructure is mainly related to the Ostwald ripening mechanism, when small grains gradually dissolve and large ones grow. This mechanism is implemented both for cobalt-rich and cobalt-depleted grains.

It should be noted that the particles on the surface and the crystalline cobalt grains, concentrated in the film thickness, exchange substance upon a transition to the late stage of catalyst particle growth (Fig. 6). This process can lead to a decrease of the total substance amount concentrated in the particles on the film surface. A similar phenomenon can be

caused by the mechanism of cobalt diffusion into the silicon substrate (not considered in the present paper).

4. Conclusion

An analysis of experiments and modeling makes it possible to understand the mechanism of formation of catalyst particles (Co) during crystallization of amorphous films (Co-Zr-O). Catalyst nanoparticles form on the film surface upon an amorphous-crystalline transition. The forming cobalt-rich and cobalt-depleted crystalline phases are characterized by different atomic volume values, which leads to catalyst displacement to the surface during grain formation and growth.

Catalyst particles which form on the film surface are partially immersed in the film and are usually surrounded by cobalt-depleted grains. Rare interactions between catalyst particles do not cause their fusion because they are separated by a boundary which exists due to different lattice orientations inside the particles. The main mechanism of catalyst particle growth is the gradual growth of large grains due to the dissolution of small ones (Ostwald ripening), which ensures the gradual decrease of the total grain boundary area and energy.

Diffusional exchange of substance between particles on the film surface and grains in the film bulk may result in a decrease of the total catalyst weight on the surface. A similar effect can be also caused by the diffusion of catalyst atoms towards the boundary with the substrate or the buffer layer, which can be an efficient drain for catalyst atoms.

Funding

This work was supported by the Ministry of Science and Higher Education of the Russian Federation, project No. 0004-2022-0004. The investigations were performed in the Institute of Nanotechnology of Microelectronics of the Russian Academy of Sciences (INME RAS) using Large Scale Research Facility Complex for Heterogeneous Integration Technologies and Silicon + Carbon Nanotechnologies.

Conflict of interest

The authors declare that they have no conflict of interest.

References

[1] K. Dasgupta, J.B. Joshi, S. Banerjee. Chem. Eng. J. **171**, 841 (2011).
[2] M. Kumar, Y. Ando. J. Nanosci. Nanotechnol. **10**, 6, 3739 (2010).
[3] S.-W. Lee, J. Han, H.I. Won, C. Young. J. Kor. Phys. Society **66**, 11, 1715 (2015).
[4] E.Z. Karimi, S.M. Zebarjad, I.A. Bataev, A.G. Bannov. Bull. Mater. Sci. **37**, 1031 (2014).
[5] M. Li, X. Liu, X. Zhao, F. Yang, X. Wang, Y. Li. Top Curr. Chem. Z **375**, 29 (2017).
[6] D.G. Gromov, S. Bulyarskii, A. Pavlov, S. Scorik, A. Shulyatév, A.Y. Trifonov. Diamond Relat. Mater. **64**, 97 (2016).
[7] S. Dubkov, A. Trifonov, E. Kitsyuk, A. Pavlov, S. Bulyarsky, S. Skorik, T. Maniecki, P. Mierczynski, D. Gromov, S. Gavrilov. J. Phys. Conf. Ser. **829**, 12002 (2017).
[8] P. Mierczynski, S.V. Dubkov, S.V. Bulyarskii, A.A. Pavlov, S.A. Gavrilov, T.P. Maniecki, D.G. Gromov. J. Mater. Sci. Technol. **34**, 472 (2018).
[9] Y. Chen, D.-H. Riu, Y.-S. Lim. Met. Mater. Int. **14**, 385 (2008).
[10] N. Provatas, K. Elder. Phase-Field Methods in Material Science and Engineering. Wiley-VCH, Weinheim (2010). 345 p.
[11] D. Fan, S. P. Chen, L.-Q. Chen. J. Mater. Res. **14**, 1113 (1999).
[12] D. Fan, L.-Q. Chen. Acta Mater.**45**, 3297 (1997).
[13] S.O. Poulsen, P.W. Voorhees, E. M. Lauridsen. Acta Mater. **61**, 1220 (2013).
[14] L. Vanherpe, N. Moelans, B. Blanpain, S. Vandewalle. Phys. Rev. E **76**, 056702 (2007).
[15] P.G.K. Amos, R. Perumal, M. Selzer, B. Nestler. J. Mater. Sci. Technol. **45**, 215 (2020).
[16] B. Nestler, H. Garcke, B. Stinner. Phys. Rev. E **71**, 041609 (2005).
[17] S.B. Biner. Programming Phase-Field Modeling. Springer, Cham. (2017).
[18] P.E. L'vov, A.R. Umantsev. Crystal Growth Des. **21**, 1, 366 (2021).